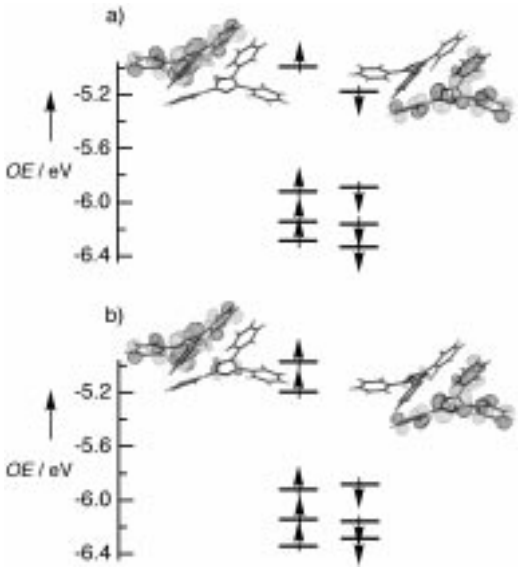

Figure 4. Molecular orbital energy level diagrams and singly occupied molecular orbitals (SOMOs) for a) the singlet state of pair B and b) the triplet state of pair B as obtained from the UB3LYP/6–31G* method. *OE* = orbital energy.

Table 1. Becke3LYP/6–31G* energies and $\langle \mathbf{S}^2 \rangle$ values for the singlet and triplet states for pair B.

Spin state	HF energy (UB + HF-LYP) [hartree]	$\langle \mathbf{S}^2 \rangle$
singlet	−2756.15237298	0.3394
triplet	−2756.15211899	2.0013

DFT calculations.[9a, d, 11] The coupling constant 2*J* was evaluated by calculating the spin-projected energy difference between the singlet and triplet states. The obtained 2*J* value of $-45\ cm^{-1}$ compares well with the experimental value of $-77\ cm^{-1}$.

In summary, we have succeeded for the first time in determining the intermolecular exchange coupling for the light-induced RP in a crystal of *o*-Cl-HABI. This study shows that DFT methods can provide an accurate description even for the through-space coupling in RPs. A combination study of X-ray diffraction and DFT calculations for the light-induced RPs in HABI derivatives will lead to a better understanding of radical-pair chemistry and solid-state reactions.

Received: July 7, 2000 [Z15412]

[1] a) M. N. Paddon-Row, *Acc. Chem. Res.* **1994**, *27*, 18–25; b) A. Rajca, *Chem. Rev.* **1994**, *94*, 871–893; c) K. Olivier, *Molecular Magnetism*, VCH, New York, **1993**; d) J. S. Miller, A. J. Epstein, *Chem. Eng. News* **1995**, *73*(40), 30–41; e) C. B. Grissom, *Chem. Rev.* **1995**, *95*, 3–24.

[2] a) T. Hayashi, K. Maeda, *Bull. Chem. Soc. Jpn*. **1960**, *33*, 565–566; b) T. Hayashi, K. Maeda, *Bull. Chem. Soc. Jpn*. **1970**, *43*, 429–438; c) D. M. White, J. Sonnenberg, *J. Am. Chem. Soc.* **1966**, *88*, 3825–3829; d) H. Tanino, T. Kondo, K. Okada, T. Goto, *Bull. Chem. Soc. Jpn*. **1972**, *45*, 1474–1480, e) X.-Z. Qin, A. Liu, A. D. Trifunac, V. V. Krongauz, *J. Phys. Chem.* **1991**, *95*, 5822–5826; f) J. V. Caspar, I. V. Khudyakov, N. J. Turro, G. C. Weed, *Macromolecules*, **1995**, *28*, 636–641.

[3] M. Kawano, T. Sano, J. Abe, Y. Ohashi, *J. Am. Chem. Soc.* **1999**, *121*, 8106–8107.

[4] a) L. R. Ryzhkov, J. M. McBride, *J. Am. Chem. Soc.* **1997**, *119*, 4826–4833; b) J. M. McBride, B. E. Segmuller, M. D. Hollingsworth, D. E. Mills, B. A. Weber, *Science* **1986**, *234*, 830–835; c) D. A. Modarelli, P. M. Lahti, C. George, *J. Am. Chem. Soc.* **1991**, *113*, 6329–6330; d) H. L. Casal, D. Griller, R. J. Kolt, F. W. Hartstock, D. M. Northcott, J. M. Park, D. D. M. Wayner, *J. Phys. Chem.* **1989**, *93*, 1666–1670.

[5] K. Okada, K. Imamura, M. Oda, M. Kozaki, Y. Morimoto, K. Ishino, K. Tashiro, *Chem. Lett*. **1998**, 891–892.

[6] Y. Teki, I. Fujita, T. Takui, T. Kinoshita, K. Itoh, *J. Am. Chem. Soc.* **1994**, *116*, 11499–11505.

[7] S. S. Eaton, M. M. Kundalika, M. S. Bhimrao, G. R. Eaton, *J. Am. Chem. Soc.* **1983**, *105*, 6560.

[8] A fit of the plot for the thermal excited triplet state was performed with the following equation: $I = \text{const.} \times (1/T) \times \exp(\Delta E/RT)/[1 + 3 \times \exp(\Delta E/RT)]$, with I = EPR intensity, T = temperature, ΔE = energy difference, R = gas constant.

[9] a) E. Goldstein, B. Beno, K. N. Houk, *J. Am. Chem. Soc.* **1996**, *118*, 6063–6043; b) E. Ruiz, P. Alemany, S. Alvarez, J. Cano, *J. Am. Chem. Soc.* **1997**, *119*, 1297–1303; c) M. Abe, W. Adam, W. M. Nau, *J. Am. Chem. Soc.* **1998**, *120*, 11304–11310; d) J. H. Rodriguez, D. E. Wheeler, J. K. McCusker, *J. Am. Chem. Soc.* **1998**, *120*, 12051–12068.

[10] For the theoretical calculations, the molecular geometry of pair B was taken from the geometry determined in the X-ray diffraction study. The spin density of the triplet RP was calculated at the UB3LYP/6–31G* level. The zfs parameter D was derived from the following dipole–dipole equation: $|D/hc| = 3\beta g(\Sigma_i \Sigma_j \rho_i \rho_j / r_{ij}^3)$, where $3\beta = 1.299\ cm^{-1}Å^3$, g is the free electron g-value, β is the Bohr magneton value, ρ_i and ρ_j are interacting spin densities, and r_{ij} is the distance between them in angstroms.[9d] No interactions were allowed between densities that belong to the same lophyl radical.

[11] S. Yamanaka, T. Kawakami, H. Nagao, K. Yamaguchi, *Chem. Phys. Lett*. **1994**, *231*, 25–33.

The First Direct Determination of a Ligand Binding Constant in Protein Crystals

Su-ying Wu, Jacqueline Dornan, George Kontopidis, Paul Taylor, and Malcolm D. Walkinshaw*

In the field of protein–ligand interactions there have been many recent attempts to predict protein–ligand dissociation constants by correlating solution binding measurements with structural features from series of protein–ligand crystal complexes.[1–6] Indeed the whole structure-based design approach relies on the assumption that the thermodynamics of binding and the structures of bound ligands in the crystal will be similar to those in the biological environment. The results presented herein provide the first evidence that this is indeed the case.

Cyclophilins provide a good template for the study of ligand binding as there is relatively little change in their backbone conformation on binding.[7] To date the only structural data on ligand complexes is for cyclosporin derivatives or proline-containing peptides.[8–10] The isoform cyclophilin 3 from *Caenorhabditis elegans* (ceCyp3) was selected as the template

[*] Prof. Dr. M. D. Walkinshaw, Dr. S.-y. Wu, J. Dornan, Dr. G. Kontopidis, Dr. P. Taylor
Structural Biochemistry Group
Institute of Cell and Molecular Biology
The University of Edinburgh
Michael Swann Building, King's Buildings
Mayfield Road, Edinburgh, EH9 3JR (UK)
Fax: (+44) 131-650-7055
E-mail: M.Walkinshaw@ed.ac.uk

  1433-7851/01/4003-0582 $ 17.50+.50/0

for this binding study because of the availability of high symmetry, well-diffracting crystals which were amenable to ligand-soaking experiments. The enzymatic properties and the X-ray structure of the free form have been described.[11]

Solution binding and inhibition of ceCyp3 by the Ala-Pro ligand was measured by its ability to inhibit peptidylprolyl isomerase (PPIase) activity. The peptidylprolyl imide bond can adopt *cis* and *trans* conformations and the assay depends on the fact that chymotrypsin can only cleave the imide bond of the chromogenic prolyl substrate when it is in the *trans* conformation. The PPIase activity of cyclophilins catalyzes the rotation about this imide bond, thus speeding up the rate at which the *cis*–*trans* equilibrium is reached.[12, 13] Ala-Pro acts as a weak inhibitor of the PPIase activity, with a measured K_d value of 23.3 mM (Figure 1).

To measure the binding constant of the Ala-Pro ligand in the crystal a series of native ceCyp3 crystals were equilibrated against different concentrations of ligand (1.2–120 mM) and the individual X-ray structures refined. X-ray refinement statistics for the structures are given in Table 1. The refined structure of the crystal soaked in 120 mM Ala-Pro shows a well-defined ligand structure with seven hydrogen bonds involved in the ligand–protein binding (Figure 2b). The guanidino group of Arg62 adopts a very different orientation to that in the native structure and displaces water molecule W_d which is present in the native structure (Figure 2a). A further three water molecules (W_a, W_b, and W_c) present in the native structure are also displaced by the Ala-Pro ligand. All other residues around the binding site, with the exception of Arg62, adopt an identical conformation to that found in the native structure.

The (2Fo-Fc) electron density maps around the binding site of ceCyp3 complexed with different concentrations of Ala-Pro provide a graphic illustration of the conversion of the native to the ligand-bound structure (Figures 3a–g). The crystal soaked in a 120 mM solution of the ligand (Figure 3g) and the native crystal (Figure 3a) provide pictures of the two extremes. The five structures soaked with intermediate

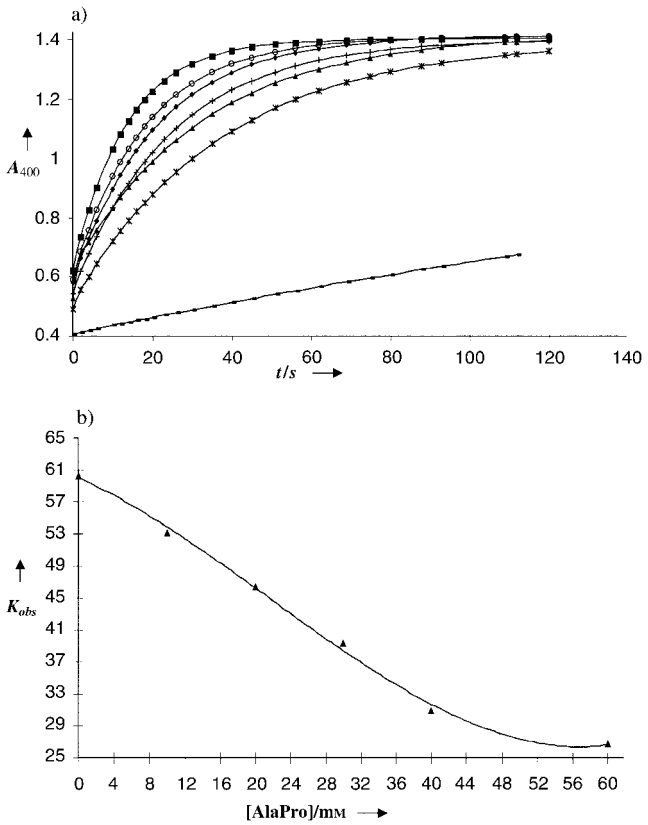

Figure 1. a) Inhibition of PPIase activity of ceCyp3 with increasing concentrations of Ala-Pro. Absorbance values were collected every 0.1 s over 2 min. The protein concentration was 20 nM and concentrations of Ala-Pro ranging between 0 and 60 mM were added. b) Determination of the K_d value for PPIase inhibition of ceCyp3 by Ala-Pro. Initial velocities from Figure 1a were used to determine k_{obsd} ($k_{obsd} = v/[S]$), where v is the velocity and [S] is the substrate concentration.[15] A plot of k_{obsd} against inhibitor concentration gives an Ala-Pro concentration of 23.3 mM for 50% inhibition. This IC_{50} value can be taken as an estimate for K_d by using $K_d = [E][L]/[EL]$ and at 50% inhibition $[E] = [EL] = 0.5[E]_T$ (where $[E_T]$ = total protein concentration, [E] = free protein concentration, [L] = free ligand concentration, and [EL] = protein concentration bound to ligand). With a large excess of ligand, the assumption $[L]_{50\%} = [L] \approx [L]_T$ can be made. At the point at which half maximal inhibition occurs $[EL] = [E]$ and $K_d = [L]_T$.

Table 1. Crystallographic statistics of the seven ceCyp3 structures.[a]

Data collection statistics	Native	1.2 mM Ala-Pro	6 mM Ala-Pro	18 mM Ala-Pro	36 mM Ala-Pro	60 mM Ala-Pro	120 mM Ala-Pro
space group, $P4_12_12$	$a=b=60.60$ Å $c=123.1$ Å $\alpha=\beta=\gamma=90°$	$a=b=60.87$ Å $c=122.99$ Å $\alpha=\beta=\gamma=90°$	$a=b=60.74$ Å $c=122.72$ Å $\alpha=\beta=\gamma=90°$	$a=b=61.03$ Å $c=122.7$ Å $\alpha=\beta=\gamma=90°$	$a=b=61.42$ Å $c=122.47$ Å $\alpha=\beta=\gamma=90°$	$a=b=61.05$ Å $c=122.67$ Å $\alpha=\beta=\gamma=90°$	$a=b=61.03$ Å $c=122.66$ Å $\alpha=\beta=\gamma=90°$
resolution range	20–1.8 Å	25–2.1 Å	25–2.0 Å	20–1.9 Å	20–1.9 Å	25–2.0 Å	20–1.9 Å
number of reflections measured	145422	165474	189319	146663	224150	270345	152448
number of unique reflections	22053	14262	16311	19030	19185	16443	19230
completeness	97.0%	98.9%	99.7%	98.6%	99.5%	95.8%	97.6%
multiplicity	6.59	11.60	11.60	7.70	11.60	16.44	7.92
R_{merge} (outer shell)	8.3% (27.8%)	9.9% (36.2%)	8.1% (31.5%)	6.7% (34.6%)	7.2% (31.3%)	7.1% (33.2%)	7.9% (33.2%)
$I/\sigma(I)$ (outer shell)	11.7 (2.60)	12.50 (3.36)	14.88 (3.62)	13.88 (2.34)	14.89 (2.90)	14.44 (2.09)	12.85 (2.13)
R_{final} ($F>4\sigma$)	20.81% (19.69%)	17.65% (16.52%)	18.08% (17.09%)	20.93% (19.44%)	19.49% (18.32%)	22.56% (19.95%)	18.26% (17.3%)
R_{free} ($F>4\sigma$)	28.47% (26.61%)	25.94% (24.97%)	26.57% (24.45%)	29.58% (27.20%)	26.84% (24.62%)	29.16% (26.37%)	25.05% (23.77%)
rms deviations from ideal geometry							
bond lengths [Å]	0.031	0.030	0.030	0.030	0.031	0.030	0.030
angle distance [Å]	0.026	0.027	0.027	0.027	0.027	0.025	0.028
mean B-factor [Å^2]	30.37	33.70	31.93	32.73	30.95	35.84	31.36

[a] $R_{merge} = \Sigma_h |I - \langle I \rangle| / \Sigma_h |I|$, where $\langle I \rangle$ is the mean intensity of all observations of reflection $h = hkl$, $\sigma(I)$ is the standard deviation of the measured intensity, and R_{free} is calculated with 5% of the data omitted from refinement for cross-validation.

  1433-7851/01/4003-0583 $ 17.50+.50/0

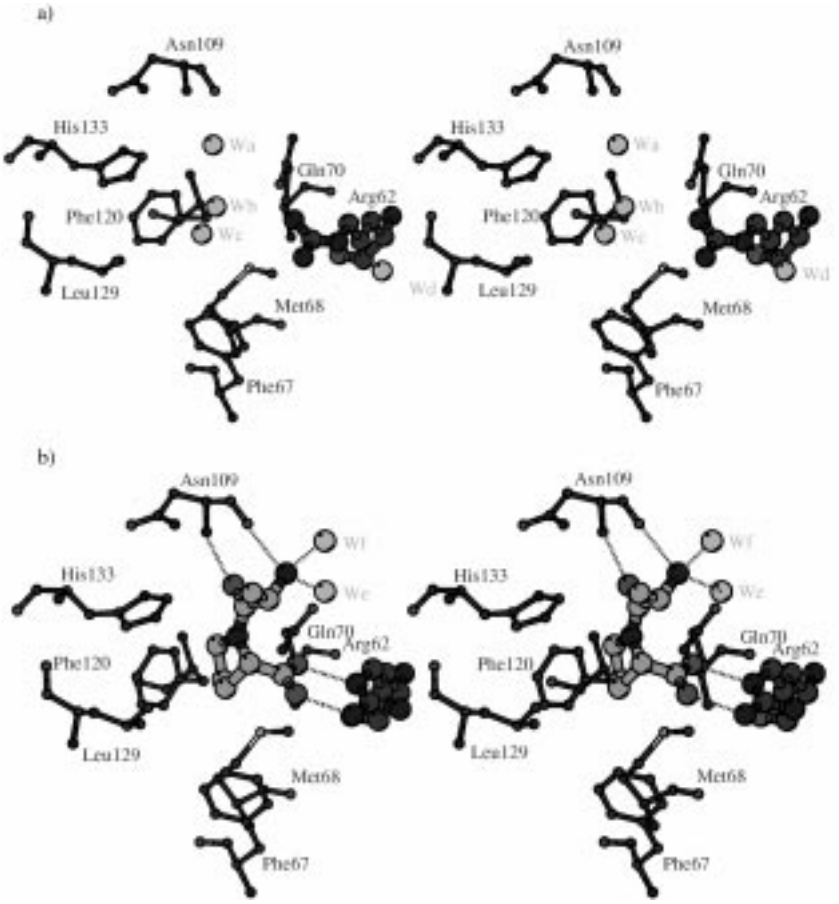

Figure 2. Active site of the structures with and without ligand. a) Stereoview of the active site of native (free) ceCyp3. The four water molecules in the active site ($W_a - W_d$) are coloured light gray. The side chain of Arg62 adopts a different conformation on ligand binding and is highlighted. b) Stereview of the active site of ceCyp3 after soaking in a 120 mM solution of Ala-Pro. The seven hydrogen bonds formed by the ligand to N/Asn109, NH_2/Arg62, W_e, O/Asn109, NE/Arg62, W_f, and NE2/Gln70 are shown as dotted black lines.

concentrations of Ala-Pro can be refined as mixtures of these two extreme structures. For example, the electron density maps of the crystals obtained in 18 mM and 36 mM solutions of the ligand (Figures 3d, e) show electron density that can clearly be interpreted as a mixture of the ligand-bound and free structures. The partial occupancy of the ligand (Q_l) is defined as the fraction of the protein molecules in the crystal occupied by the Ala-Pro ligand. Q_n is the fraction of protein molecules in the crystal in the native (free) state. As each molecule in the crystal must be in one of these states then $Q_n + Q_l = 1$. With this simple two-state model, occupancies can be constrained in the following way. The occupancy of the ligand (Q_l) is the same as the occupancy of the $Arg62_{(l)}$ in its ligand-bound conformation while the occupancy of the native

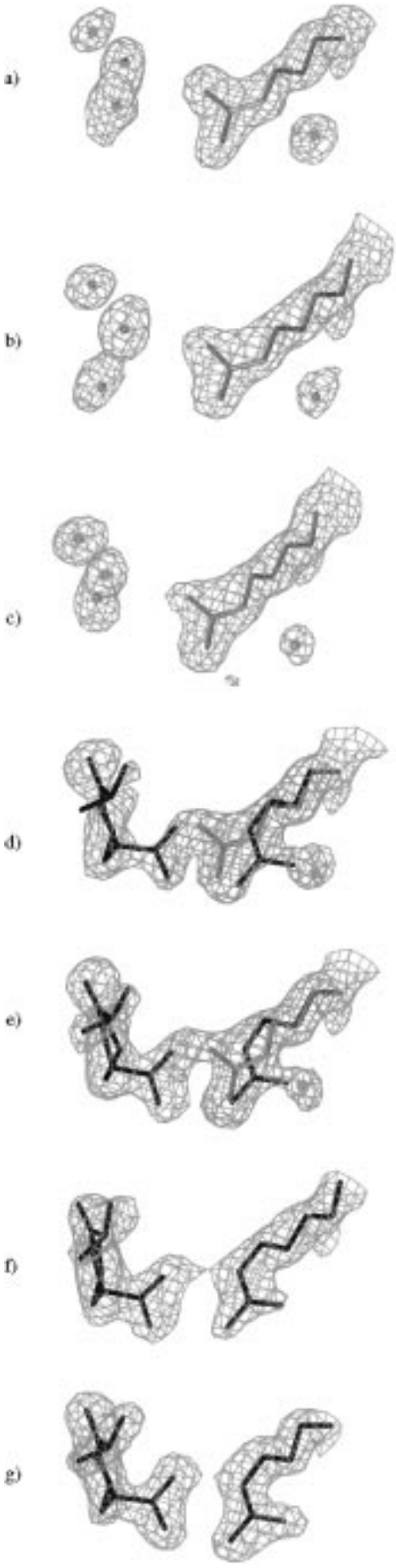

Figure 3. Difference electron density maps of crystals soaked with increasing ligand concentration. The (2Fo-Fc) maps highlighting the ligand, Arg62, and water molecules in the active site are contoured at 1.5 sigma using the program O.[16] a) The native ceCyp3 structure shows the density of the water molecules. b) and c) The crystals were soaked in 1.2 mM and 6 mM Ala-Pro, respectively. The electron density contoured at 1.5 sigma looks almost identical to the native structure. d) and e) The crystals were soaked in 18 mM and 36 mM Ala-Pro, respectively, and can be clearly interpreted as having features of both the native (light gray) and ligand-bound (black) forms. f) and g) The crystals were soaked in 60 and 120 mM Ala-Pro, respectively. The electron density contoured at 1.5 sigma shows only features corresponding with the fully ligand-bound form.

  1433-7851/01/4003-0584 $ 17.50+.50/0

structure (Q_n) is the occupancy of $Arg62_{(n)}$ in the native conformation, which must be the same as the occupancy of the water molecules W_a, W_b, W_c, and W_d. These occupancy constraints can be conveniently applied using the refinement programme SHELX97,[14] and the fractional occupancies refined. The occupancy is in fact only one parameter: $Q_l = 1 - Q_n$.

By regarding the crystal soaking experiment as a simple equilibrium in which each protein molecule in the crystal lattice can be bound or free, the fractional occupancy can be related to the dissociation constant in the following way:

$[PL] \rightarrow [P] + [L]$

$K_{cd} = [P][L]/[PL]$

$[P]_{total} = [PL] + [P]$

$[PL] = [P]_{total} Q_l$

$[P] = [P]_{total}(1 - Q_l)$

Thus,

$K_{cd} = \{[P]_{total}(1 - Q_l)\}[L]/[P]_{total} Q_l = (1 - Q_l)[L]/Q_l$

$Q_l/Q_n = [L]/K_{cd}$

where

K_{cd} is the crystal dissociation constant, [P] is the concentration of free protein, [L] is the concentration of the ligand (it is assumed that the concentration of ligand in the 10 μL drop is constant throughout the soaking experiment), [PL] is the concentration of protein with ligand, $[P]_{total}$ is the total concentration of protein, Q_l is the occupancy of ligand (fraction of the protein sites in the crystal occupied by ligand), Q_n is the fraction of the protein sites in the free state ($=(1 - Q_l)$).

A value of 26.8 mM was obtained for K_{cd} as calculated from the slope of the plot of (Q_l/Q_n) versus [L] (Figure 4b). This value is in close agreement with the inhibition constant of 23.3 mM measured for the Ala-Pro ligand in solution using the PPIase assay. It is noteworthy that the quality and information content of the X-ray data is sufficient to accurately refine the partial occupancy of the ligand-bound structures even when visual inspection of the electron density maps suggests the electron density is dominated by one of the (native or ligand-bound) forms. In general, interpreting a structure with such low partial occupancy would be almost impossible using conventional map-fitting methods without a well-refined native structure being available. Indeed inspection of the series of electron density maps shown in Figure 3 suggests that, without prior knowledge, side-chain conformations with occupancies less than about 20% would not be readily apparent in electron density maps.

In protein–ligand complexes it can frequently be difficult to distinguish water molecules or disordered water molecules from a weakly bound ligand. A helpful feature of this system is the movement of the Arg62 side chain on ligand binding, as this gives an excellent double-check on the ligand occupancy. In a separate experiment we also showed that diffusion and binding of the ligand in this system took place on a timescale of seconds. A crystal soaked in 120 mM ligand solution for 60 seconds was flash frozen and the refined structure shown to be identical to that from a crystal soaked for 17 hours. The kinetics of ligand–protein binding is likely to vary somewhat from crystal to crystal depending on the crystal packing, solvent channel size, and ligand size. However, we suggest that

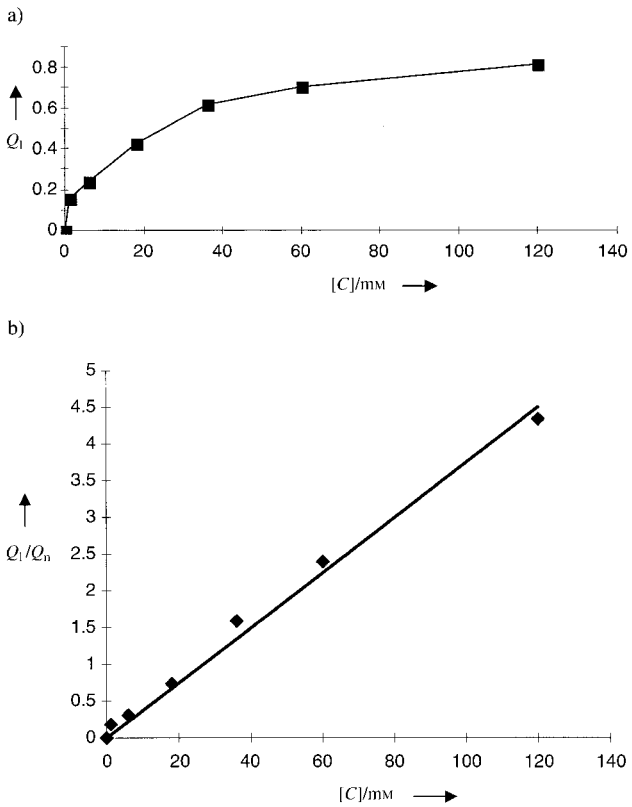

Figure 4. a) Refined occupancy for the seven different crystal structures. Each point on the curve represents the occupancy of the Ala-Pro ligand as determined from an X-ray refinement of a crystal soaked in a given concentration of Ala-Pro.[17] The ligand concentrations used in the soaking experiments were 0, 1.2, 6, 18, 36, 60, and 120 mM. The corresponding occupancies obtained from crystallographic refinement were 0, 0.155, 0.238, 0.424, 0.613, 0.705, and 0.812. b) Plot of ligand concentration against Q_l/Q_n. Q_l: occupancy of ligand (fraction of the protein sites in the crystal occupied by ligand), Q_n: fraction of the protein sites in the free state ($=(1 - Q_l)$). The ligand occupancies of the different crystals were measured by crystallographic refinement as described in the text. The experimental data fit the theoretical line with a high R^2 value of 0.990 and a slope $1/K_{cd} = 0.0373$. This gives a value for K_{cd} (the crystal dissociation constant) of 26.8 mM.

for a large number of proteins, this crystallographic method of measuring binding constants could be developed into a relatively efficient and routine technique.

Experimental Section

Crystallization and data collection: CeCyp3 was crystallized at 16 °C by the hanging drop vapour-diffusion method using 29–31% poly(ethylene glycol) methyl ether 5000 (MPEG 5000) as precipitant.[11] Native ceCyp3 crystals (approximately $0.2 \times 0.3 \times 0.3$ mm) were soaked in six 10 μL drops of well solution containing the Ala-Pro dipeptide at 1.2, 6, 18, 36, 60, and 120 mM, respectively. Crystals were soaked for between 17 and 27 hours.

The composition of the cryoprotectant was glycerol (0.2 mL), MPEG 5000 (0.7 mL), 1.0 M sodium citrate/citric acid (0.1 mL, pH 5.6). Crystals were mounted in a 0.2–0.3-mm cryoloop (Hampton Research, Inc.), dipped in cryoprotectant for a few seconds, and frozen by plunging into liquid nitrogen. The frozen crystal was then transferred to a magnetic goniometer head in a stream of nitrogen at 100 K. All diffraction data were collected on a 300-mm MarResearch imaging plate system mounted on an ENRAF Nonius FR571 rotating anode generator operating at 40 kV, 80 mA, and producing $Cu_{K\alpha}$ radiation from a graphite crystal monochromator.

Refinement: The ceCyp3 native structure was used as a starting model. Positional and B-factor refinement were performed using SHELX97

  1433-7851/01/4003-0585 $ 17.50+.50/0

(Table 1). The coordinates of $Arg62_{(n)}$, $Arg62_{(l)}$, Ala-Pro, W_a, W_b, W_c, and W_d were fixed during occupancy refinement. $Arg62_{(n)}$ represents the Arg62 conformation without Ala-Pro bound and $Arg62_{(l)}$ represents the Arg62 conformation with Ala-Pro bound to ceCyp3. The B-factors of $Arg62_{(n)}$, W_a, W_b, W_c, and W_d were fixed to the same B-factor values as those of the native structure. Individual atomic B-factors for $Arg62_{(l)}$ and Ala-Pro were refined together with occupancy (Figure 4). The restraints applied in the occupancy refinement are summarized below:

$$Q_{Arg62(n)} + Q_{Arg62(l)} = 1$$

$$Q_{Arg62(l)} = Q_l$$

$$Q_{Arg62(n)} = Q_{Wa} = Q_{Wb} = Q_{Wc} = Q_{Wd}$$

where

$Q_{Arg62(n)}$: is the occupancy of the Arg62 conformation with no Ala-Pro binding, $Q_{Arg62(l)}$: is the occupancy of the Arg62 conformation with Ala-Pro binding, and Q_l: is the occupancy of Ala-Pro.

PPIase assay:[13] α-chymotrypsin selectively hydrolyzes the C-terminal *p*-nitroanilide bond of the substrate in the *trans* X-Pro conformer only. This hydrolysis releases the chromophore 4-nitroaniline, the accumulation of which is recorded by measuring the absorbance at 400 nm as a function of time. Substrate (*N*-succinyl-Ala-Ala-Pro-Phe-p-nitroanilide, Bachem AG) was dissolved in LiCl/2,2,2-trifluoroethanol (LiCL/TFE) to give a stock solution of 100 mM. The experiment took place at 4 °C. Constant temperature was maintained within the cuvette by a Peltier (PTP-1) temperature control unit. A Perkin – Elmer UV/Vis Lambda 20 spectophotometer was used.

Proteins: ceCyp3 solution was freshly prepared before the experiment from frozen stock solution, at the appropriate concentration, by dilution in buffer 50 mM 2-[4-[2hydroxyethyl)-1-piperazinyl]ethanesulfonic acid (HEPES), 100 mM NaCl, pH 8.0 (buffer A).

α-chymotrypsin (Sigma): In a typical experiment 10 µL of 20 nM ceCyp3 was made up to 870 µL with buffer A and the appropriate volume of Ala-Pro in a 1-mL cuvette. The cuvette was then preincubated for 30 min on ice. Immediately before the assay, 100 µL of chymotrypsin solution (50 mg mL^{-1} in 10 mM HCl) was added, followed by 30 µL of a 3.7 µM stock solution of Suc-Ala-Ala-Pro-PNA in LiCl (470 mM)/TFE. The reaction progress was monitored by the absorbance change at 400 nm that accompanies the hydrolysis of the amide bond and the release of 4-nitroaniline.

Received: September 8, 2000 [Z15779]

[1] B. M. Baker, K. P. Murphy, *Methods Enzymol.* **1998**, *295*, 294 – 315.
[2] B. K. Shoichet, A. R. Leach, I. D. Kuntz, *Proteins* **1999**, *34*, 4 – 16.
[3] G. M. Verkhivker, P. A. Rejto, D. Bouzida, S. Arthurs, A. B. Colson, S. T. Freer, D. K. Gehlhaar, V. Larson, B. A. Luty, T. Marrone, P. W. Rose, *J. Mol. Recognit.* **1999**, *12*, 371 – 389.
[4] M. Schapira, M. Totrov, R. Abagyan, *J. Mol. Recognit.* **1999**, *12*, 177 – 190.
[5] M. D. Eldridge, C. W. Murray, T. R. Auton, G. V. Paolini, R. P. Mee, *J. Comput. Aided Mol. Des.* **1997**, 11, 425 – 445.
[6] H. J. Bohm, *J. Comput. Aided Mol. Des.* **1998**, *12*, 309 – 323.
[7] P. Taylor, H. Husi, G. Kontopidis, M. D. Walkinshaw, *Prog. Biophys. Mol. Biol.* **1997**, *67*, 155 – 181.
[8] J. Kallen, M. D. Walkinshaw, *FEBS Lett.* **1992**, *300*, 286 – 290.
[9] J. Kallen, V. Mikol, P. Taylor, M. D. Walkinshaw, *J. Mol. Biol.* **1998**, *283*, 435 – 449.
[10] Y. D. Zhao, H. M. Ke, *Biochemistry* **1996**, *35*, 7362 – 7368.
[11] J. Dornan, A. P. Page, P. Taylor, S. Y. Wu, A. D. Winter, H. Husi, M. D. Walkinshaw, *J. Biol. Chem.* **1999**, *274*, 34 877 – 34 883.
[12] D. Kern, G. Kern, G. Scherer, G. Fischer, T. Drakenberg, *Biochemistry* **1995**, *34*, 13 594 – 13 602.
[13] J. L. Kofron, P. Kuzmic, V. Kishore, E. Colonbonilla, D. H. Rich, *Biochemistry* **1991**, *30*, 6127 – 6134.
[14] G. M. Sheldrick, SHELX97, University of Göttingen, **1997**.
[15] J. Liu, C. T. Walsh, *Proc. Natl. Acad. Sci. USA* **1990**, *87*, 4028 – 4032.
[16] T. A. Jones, J. Y. Zou, S. W. Cowan, M. Kjeldgaard, *Acta Crystallogr. Sect. A* **1991**, *47*, 110 – 119.
[17] Crystallographic data for the structures reported in this paper have been deposited with the Protein Data Bank as supplementary publication no. PDB-1E8K (see http://www.rcsb.org/pdb/index.html).

A Heterogeneous *cis*-Dihydroxylation Catalyst with Stable, Site-Isolated Osmium – Diolate Reaction Centers**

An Severeyns, Dirk E. De Vos, Lucien Fiermans, Francis Verpoort, Piet J. Grobet, and Pierre A. Jacobs*

Osmium tetroxide is by far the most versatile catalyst for *cis*-dihydroxylation (DH) of double bonds.[1, 2] When homogeneous catalysts are used, free OsO_4 is always present in some step of the catalytic cycle, and the high toxicity and volatility of OsO_4 have hitherto obstructed industrial application. Previous attempts to immobilize OsO_4 used polymers, for example, with coordination of OsO_4 on polyvinylpyridine.[3, 4] However, hydrolysis of the intermediate Os^{VI} diolate complex requires that Os is detached from the polymeric Lewis base,[5] and this implies an inherent liability to Os leaching. Similarly, reports on immobilized alkaloids for asymmetric DH mention that Os leaching necessitates Os supplementation in subsequent runs.[6] In another attempt, OsO_4 was entrapped in polystyrene microspheres, but the mechanism by which OsO_4 is retained within the polymer is not understood.[7] Herein we report a solid with Os^{VIII} type reactivity, and with a persistent bond between Os and the support. Rigorous heterogeneity tests and reactions with 12 olefins substantiate the value of the new Os catalyst.

Our approach is rooted in the mechanism of the *cis*-dihydroxylation, which comprises two stages: 1) attack of the Os^{VIII} *cis*-dioxo complex on the olefin (osmylation), 2) reoxidation of Os^{VI} to Os^{VIII} and hydrolytic release of the diol. Two points are particularly relevant. First, if the hydrolytic conditions are not too drastic, *tetrasubstituted* olefins are not converted into *cis*-diols.[8, 9] These olefins are smoothly osmylated to an osmate(VI) ester, but the rate of subsequent hydrolysis is zero (0% yield for a tetrasubstituted olefin vs. 83% for a trisubstituted olefin, ref. [8]). Second, an Os^{VI} monodiolate complex can be reoxidized to *cis*-dioxo Os^{VIII} without release of the diol; subsequent addition of a second olefin results in an Os bisdiolate complex.[10] These two properties make it possible to immobilize a catalytically active Os compound by the addition of OsO_4 to a tetrasubstituted olefin that is covalently linked to a silica support (**1a**, Scheme 1). The tetrasubstituted diolate ester (**1b**) which is

[*] Prof. Dr. Ir. P. A. Jacobs, Ir. A. Severeyns, Prof. Dr. Ir. D. E. De Vos, Prof. Dr. P. J. Grobet
Center for Surface Chemistry and Catalysis
Katholieke Universiteit Leuven
Kardinaal Mercierlaan 92, 3001 Heverlee (Belgium)
Fax: (+32) 16-32-1998
E-mail: pierre.jacobs@agr.kuleuven.ac.be
Prof. Dr. L. Fiermans
Laboratory for Crystallography and Study of Solid Matter
Universiteit Gent (Belgium)
Prof. Dr. F. Verpoort
Deptment of Inorganic and Physical Chemistry
Universiteit Gent (Belgium)

[**] This work was supported by the Belgian Federal Government in the frame of an Interuniversitary Attraction Pole on Supramolecular Catalysis. We are indebted to FWO for fellowships (A.S., D.D.V.) and for a research grant (D.D.V., F.V., P.A.J.).

  1433-7851/01/4003-0586 $ 17.50+.50/0